KIGAS Vol.7, No.3, September, 2003
(Journal of the Korean Institute of Gas)

비예혼합 대향류 화염의 축대칭 모사
- 연료농도가 화염구조에 미치는 영향 -

†박 외 철
부경대학교 공과대학 안전공학과
(2003년 7월 22일 접수, 2003년 9월 19일 채택)

Axisymmetric Simulation of Nonpremixed Counterflow Flames
- Effects of Fuel Concentration on Flame Structure -

Woe-Chul Park
Department of Safety Engineering, Pukyong National University, Busan 608-739, Korea
(Received 22 July 2003 ; Accepted 19 September 2003)

요 약

연료농도에 따른 대향류 화염구조의 변화를 조사하고 수치법을 검증하기위해, 축대칭 메탄-공기 대향류화염을 모사하였다. 변형률 a_g=20, 60, 90 s^{-1}과 연료 중 메탄의 몰분율 x_m=20, 50, 80%를 수치매개변수로 하여, 변형율과 연료농도에 따라 온도분포, 닥트 중심축의 온도분포와 축방향 속도의 분포를 계산하였다. 축대칭 모사는 혼합분율 연소모델을 채용한 FDS로 수행하였고, 계산결과를 구체적 화학반응을 포함한 1차원 화염코드 OPPDIF의 계산결과와 비교하였다. 본 연구에서 조사한 모든 변형율과 연료농도에서 축대칭 모사의 온도 및 축방향 속도 분포가 1차원 계산결과와 잘 일치하는 것으로 나타났다. 연료농도가 증가하면 화염의 두께와 최고온도가 증가하고 반경이 감소함을 알 수 있었다.

Abstract - The axisymmetric methane-air counterflow flame was simulated to investigate changes in the flame structure due to the fuel concentration and to evaluate the numerical method. The global strain rates a_g= 20, 60, 90 s^{-1} and the mole fractions of methane x_m= 20, 50 and 80% in the fuel stream were taken to be numerical parameters. The axisymmetric simulation was conducted by using the Fire Dynamics Simulator (FDS) which employed a mixture fraction combustion model, and the results were compared with those of OPPDIF, which is an one-dimensional flamelet code and includes detail chemical reactions. In all the cases tested, there was good agreement in the temperature and axial velocity profiles between the axisymmetric and one-dimensional simulations. It was shown that the flame thickness and peak flame temperature increase and the flame radius decreases as the fuel concentration increases.

Key words : methane-air counterflow flame, microgravity, fuel concentration, global strain rate, peak flame temperature, flame thickness, flame radius

I. INTRODUCTION

Understanding the structure and extinction mechanism of diffusion flames is important in development of fire suppression agents. The nonpremixed

†주저자 : wcpark@pknu.ac.kr

counterflow flame obtained from a simple experimental apparatus has been studied for fire suppression agents (e.g., Hamins et al.[1]). OPPDIF[2], a program for computing opposed-flow diffusion flames and a part of CHEMKIN[3], and an one-dimensional flamelet code based on a similarity solution by neglecting buoyancy, has been utilized in many counterflow flame studies (e.g., Maruta et al.[4]). Although it provides results of complex chemical reactions including species mass fraction, information on the axisymmetric flame is not available. OPPDIF is applicable to problems where bouyancy is negligible such as in microgravity conditions. Meanwhile the Fire Dynamics Simulator(FDS)[5], developed for three-dimensional transient fire simulations, provide information on flame structure such as flame shape and temperature distribution in multidimensional situations. Park[6] applied FDS with a direct numerical simulation to the methane-air counterflow flame and showed that FDS is capable of predicting the counterflow flames in normal and zero gravity. Further evaluation of the method in a wide range of fuel concentration is in need. The objectives of this study are, through the axisymmetric simulations by using FDS, to investigate the counterflow flame structure for fuel concentrations, and to evaluate FDS further. Comparisons were made between the results of FDS and those of OPPDIF. The effects of fuel concentration on the flame thickness and its radius were also investigated.

II. METHODOLOGY

The counterflow burner has two opposing ducts separated by 15 mm as shown in Fig. 1. The fuel is supplied through the fuel duct, and air flows in the oxidizer duct. The diameter of each duct is 15 mm, and its thickness is 0.5 mm. Combustion takes place in quiescent nitrogen gas. The oxidizer is pure air, and the fuel is composed of a mixture of methane and nitrogen.

The top hat velocity profile[7] was imposed at the duct exits, and the no slip condition on the duct walls. The temperature of the fuel and air streams was set to 25°C. Since the results obtained by axisymmetric simulations with FDS are compared with those of OPPDIF[2] in which buoyancy is neglected, the gravity was set to zero in FDS, The radiation loss was not included in both FDS and OPPDIF since it is small[4].

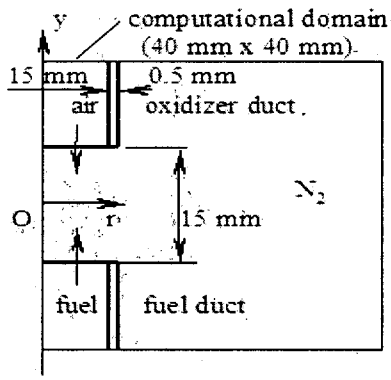

Fig. 1 The counterflow burner and computational domain.

Following the previous study of Park[1], the computational domain was taken to be 40 mm x 40 mm, and a uniform grid spacing of 0.5 mm x 0.5 mm. Since a steady state flame was obtained in about 0.7 s, the average temperature and axial velocity along the centerline(y-axis) were calculated from the instantaneous values of 0.8-1.0 s. The solution procedures are described in McGrattan et al.[5] and Park and Hamines[6].

For given global strain rate a_g, and fuel concentration x_m, the air velocity V_A and the fuel velocity V_F at the duct exits are calculated from the definition of the global strain rate, $a_g=-2V_A[1-V_Fr_F^{0.5}/V_Ar_A^{0.5}]/L$,

where $V_A = -V_F$, r_A is the density of air, and r_F is the density of the fuel (methane and nitrogen mixture) at 1 atm and 25°C. Computations were carried out for each combination of the two numerical parameters, the strain rate of a_g= 20, 60, 90 s^{-1}, and the mole fraction of methane in the fuel stream, x_m= 20, 50, 80%.

III. RESULTS AND DISCUSSION

3.1 a_g= 20 s^{-1}

The flames at a_g= 20 s^{-1}, obtained by FDS, are compared for the mole fracion of CH_4 in the fuel stream, x_m= 20% and 80% in Fig. 2. The flame of the richer fuel concentration is thicker and the flame radius is smaller compared with the flame of the leaner fuel concentration.

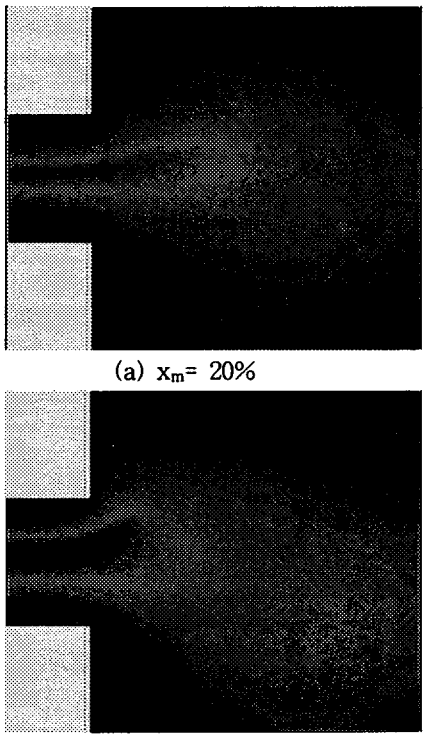

(a) x_m= 20%

(b) x_m= 80%

Fig. 2 Flames for a_g= 20 s^{-1} (FDS).

To see the changes in flame thickness and radius with the fuel concentration more clearly, the isotherms were plotted in Fig. 3. Each line is of 100°C increment. The innermost isotherm, which represents 1000°C, shows that increasing the mole fraction of methane increases the flame thickness, but decreases the flame radius. Note that comparisons of the flame shape or isotherms between FDS and OPPDIF are not possible since OPPDIF simulates the flame in one-dimension only.

In Fig. 4, the profiles of temperature and axial velocity along the duct centerline (y-axis in Fig. 1) for x_m= 20, 50 and 80% at a_g= 20 s^{-1} were compared between FDS and OPPDIF. Both the temperature and axial velocity are in excellent agreement except for the temperature of x_m= 80%.

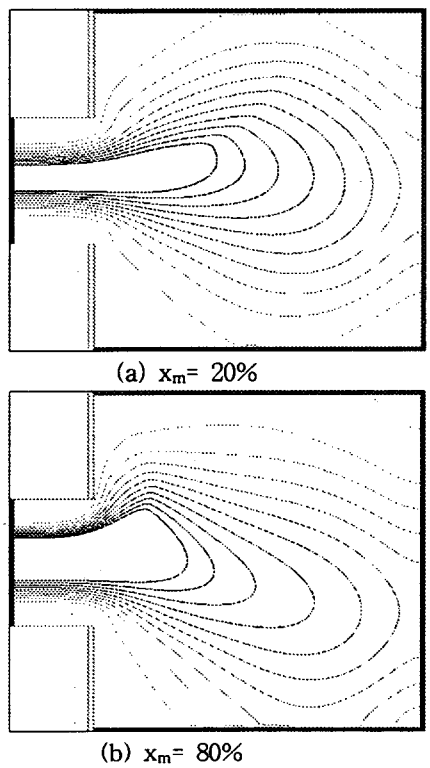

(a) x_m= 20%

(b) x_m= 80%

Fig. 3 Isotherms for a_g= 20 s^{-1}(FDS).

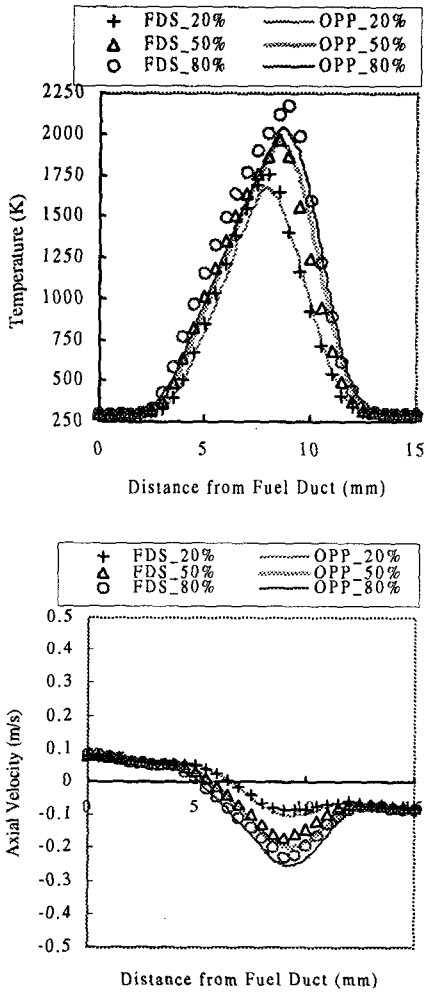

Fig. 4 Comparison of temperature and axial velocity profiles for a_g= 20 s^{-1}.

The theoretical peak flame temperature is 2227 K[8], and FDS predicted 2200 K while OPPDIF did 2062 K for the undiluted methane (x_m= 100%). This may imply that the higher peak temperature of FDS is better predicted compared with OPPDIF. The temperature profiles also show that the peak flame temperature increases with the fuel concentration and that the flame position slightly moves towards the upper oxidizer duct with x_m.

3.2 a_g= 60 s^{-1}

Fig. 5 compares the flames for x_m= 20% and 80% at a_g= 60 s^{-1}. The fuel-rich flame is thicker and the flame radius is smaller than the fuel-lean flame.

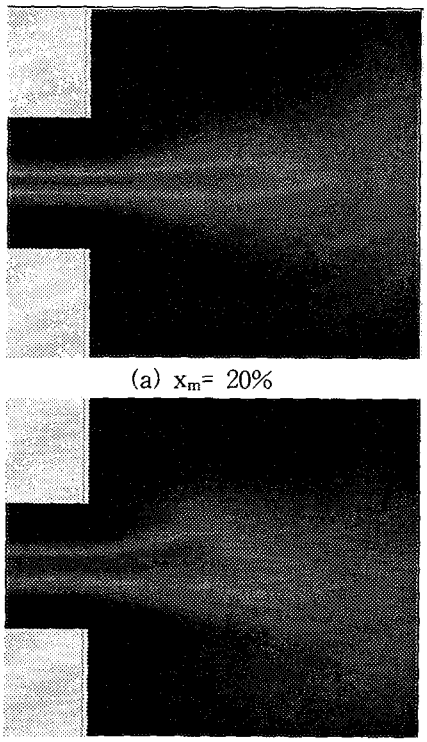

(a) x_m= 20%

(b) x_m= 80%

Fig. 5 Flames for a_g= 60 s^{-1} (FDS).

Fig. 6 depicts the isotherms of the two flames. It can be seen that the flame thickness increases and the flame radius decreases with increasing x_m from the innermost isotherm of 1000°C, similarly to the lower strain rate case of a_g= 20 s^{-1}.

Fig. 7 is the profiles of temperature and axial velocity along the duct centerline for the mole fraction of methane in the fuel stream, x_m= 20, 50 and 80%, at a_g= 60 s^{-1}. Both the temperature and axial velocity are in very good agreement between FDS and

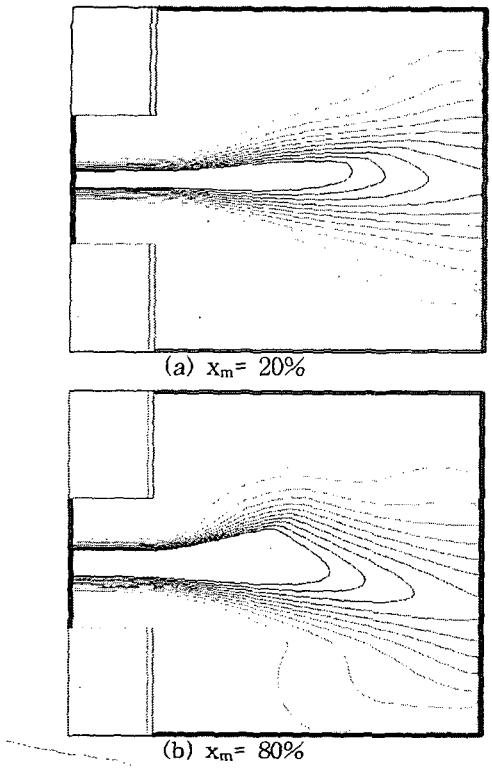

Fig. 6 Isotherms for a_g= 60 s^{-1} (FDS).

OPPDIF. The peak flame temperature of FDS is higher than that of OPPDIF, and FDS may predict it better than OPPDIF as mentioned in the case of a_g= 20 s^{-1}. It is confirmed that the peak flame temperature increases with x_m. The flame position remains at the midplane between the two ducts in spite of different x_m.

3.3 a_g= 90 s^{-1}

As shown in Figs. 8 and 9, when the strain rate is 90 s^{-1}, the flames are stretched in the radial direction more than the two lower strain rates of a_g= 20 and 60 s^{-1}. This is caused by increase in the velocity at duct exits with strain rate a_g. The variation in the flame thickness and flame radius with the mole fraction of

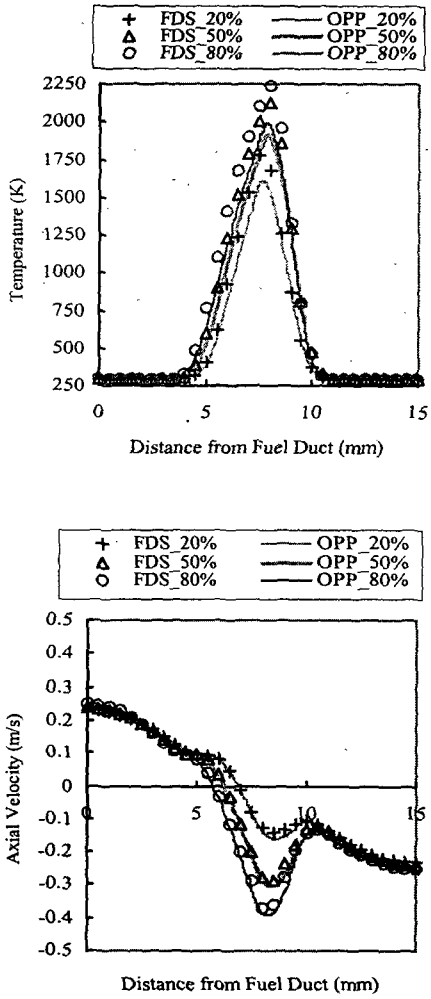

Fig. 7 Comparison of temperature and axial velocity profiles for a_g= 60 s^{-1}.

methane in the fuel stream is similar to those of the two lower strain rate cases.

The temperature profiles of FDS in Fig. 10 agree well with those of OPPDIF for the three fuel concentrations, and x_m does not change the flame position. Discrepancy in the axial velocity profiles in the high temperature region between FDS and OPPDIF is noted at x_m= 50% and 80%.

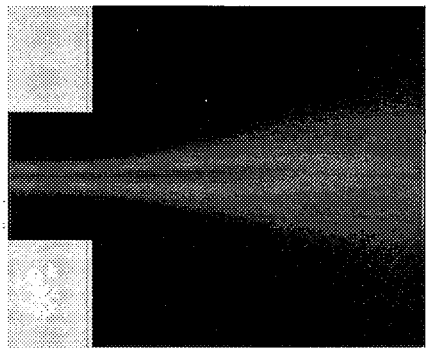

(a) x_m= 20%

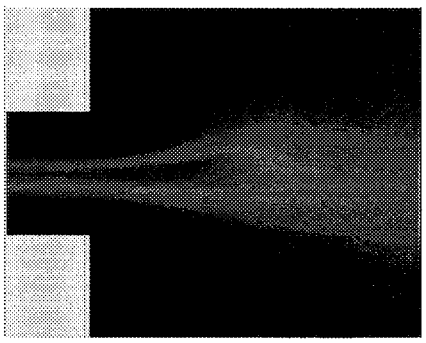

(b) x_m= 80%

Fig. 8 Flames for a_g= 90 s^{-1} (FDS).

IV. CONCLUSIONS

The flame structure of the nonpremixed nitrogen diluted counterflow methane-air flames were investigated using FDS for the mole fractions of methane in the fuel stream, 20, 50, 80% at each strain rate of 20, 60, and 90 s^{-1}. The results of axisymmetric simulations were compared with those of one-dimensional simulations with OPPDIF. The temperature and axial velocity profiles along the duct centerline of FDS agreed well with those of OPPDIF. The flames and isotherms obtained by FDS showed that increasing fuel concentration increases the flame thickness and peak flame temperature, and decreases the flame radius in all the three strain rate cases. The flame position remained unchanged at the midplane between the two ducts at moderate strain rates, a_g= 60 and 90 s^{-1}, while the flame moved slightly towards the oxidizer duct at low strain rate, a_g= 20 s^{-1}, when the fuel concentration increased.

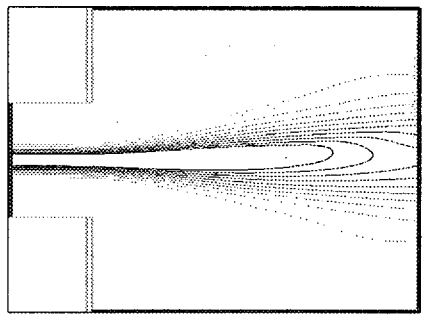

(a) x_m= 20%

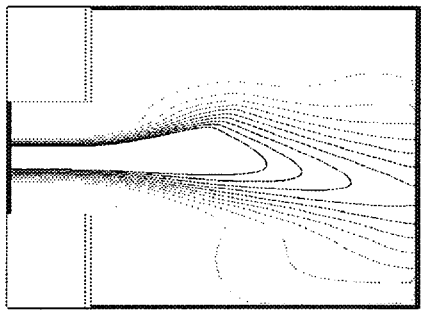

(b) x_m= 80%

Fig. 9 Isotherms of a_g= 90 s^{-1} (FDS).

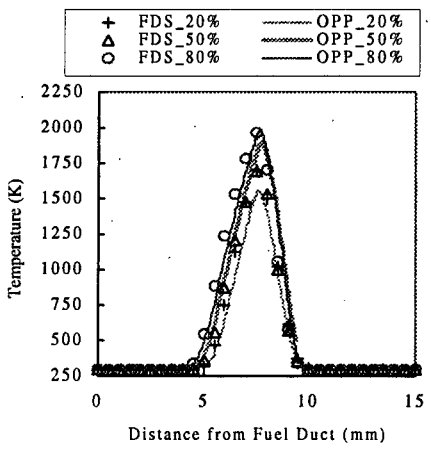

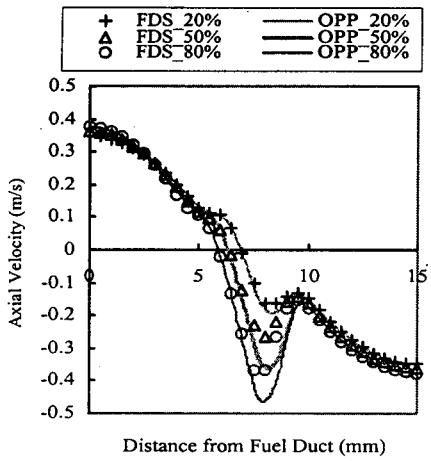

Fig. 10 Comparison of temperature and axial velocity profiles for a_g= 90 s^{-1}.

NOMENCLATURE

a_g : global strain rate, $-2V_A[1-V_F r_F^{0.5}/V_A r_A^{0.5}]/L$

L : separation distance between two ducts, 15 mm

V_A : air velocity at duct exit

V_F : fuel velocity at duct exit

x_m : fuel concentration (mole fraction of methane in fuel stream)

r_A : density of air

r_F : density of fuel

REFERENCES

[1] Hamins, A., D. Trees, K. Seshadri, and H.K. Chelliah, "Extinction of Nonpremixed Flames with Halogenated Fire Suppressants, "Combustion and Flames, Vol.99, pp.221-230 (1994).

[2] Lutz, A., R.J. Kee, J. Grcar and F.M. Rupley, "A Fortran Program Computing Opposed Flow Diffusion Flames", SAND96-8243, Sandia National Laboratories, Livermore, CA, U.S.A. (1997).

[3] http://www.reactiondesign.com.

[4] Maruta, K., M. Yoshida, H. Guo, Y. Ju and T. Niioka, "Extinction of Low-Streched Diffusion Flame in Microgravity", Combustion and Flames, 112, pp.181-187 (1998).

[5] McGrattan, K.B., H.R Baum, R.G. Rehm, A. Hamins, G.P. Forney, J.E. Floyd and S. Hostikka, Fire Dynamics Simulator Technical Reference Guide, v.3, National Institute of Standards and Technology, Gaithersburg, MD, U.S.A. (2002).

[6] Park, W.C. "An Evaluation of a Direct Numerical Simulation for Counterflow Diffusion Flames", J. Korea Institute for Industrial Safety, 16(4), pp.74-81 (2001).

[7] Park, W.C. and A. Hamins, "Investigation of Velocity Boundary Conditions in Counterflow Flames", KSME Int'l J., 16(2), pp.262-269 (2002).

[8] Baumeister, T., E.A. Avallone and T. Baumeister III, Marks' Standard Handbook for Mechanical Engineers, 8th ed., McGraw-Hill, p.4-57 (1978).